Self-similarity of damage-failure transition and the power laws of fatigue crack advance

Oleg Naimark, Vladimir Oborin, Mikhail Bannikov
Institute of Continuous Media Mechanics of Ural branch of RAS, 614013, Perm, Russia
naimark@icmm.ru, http://orcid.org/0000-0001-6537-1177
oborin@icmm.ru, http://orcid.org/0000-0003-2836-2073
mbannikov@icmm.ru, https://orcid.org/0000-0002-5737-1422

Citation: Naimark, O., Oborin, V., Bannikov, M., Self-similarity of damage-failure transition and the power laws of fatigue crack advance, Frattura ed Integrità Strutturale, 70 (2024) 272-285.

Received: 28.06.2024
Accepted: 07.09.2024
Published: 17.09.2024
Issue: 10.2024

KEYWORDS. Multiscale damage kinetics, VHCF, Defect induced criticality.

INTRODUCTION

The basic conceptions of the Finite Fracture Mechanics and the Critical Distances Theory [1] are considered in the links with the results of the statistically based thermodynamics of solid with defects and kinetics of damage-failure transition due to the metastability of free energy release and the existence of two singularities related to the stress field and damage localization kinetics in the Process Zone at the crack tip area [2]. These singularities represent intermediate asymptotic self-similar solutions and can be proposed as a physical basis of the Finite Fracture Mechanics, the nonlocality effects for the damage localization staging, small crack nucleation and crack advance in the presence of metastability of free energy release [3]. The "Critical Distances" are identified as characteristic lengths of damage localization related to the correlated dynamics self-similar collective modes of defects [4].

Two types of self-similar solutions related to the Irwin stress singularity (stress intensity factor) and damage localization kinetics as collective modes of defects are analyzed as "intrinsic" and "extrinsic" mechanisms providing the fracture scenario in the variety of loads conditions [5]. Intrinsic mechanisms are an inherent property of the material caused by the universality

scenario of damage localization related in the Process Zone [6]. They control driving forces (or stress intensities) necessary to initiate Process Zone and following cracking at the crack tip area. Intrinsic mechanisms are dominantly considered as toughening mechanisms in ductile materials associated with crack-tip plasticity.
The fatigue-crack growth has specific nature revealing the sensitivity to both intrinsic (damage) and extrinsic mechanisms which distinguishes the fatigue behavior of ductile and brittle solids. The mechanisms of fatigue-crack growth are reflected in the specific dependencies of crack growth rates da/dN on ΔK and K_{max} [7].

$$\frac{da}{dN} = C\left(K_{\max}\right)^{n}\left(\Delta K\right)^{m} \tag{1}$$

where C is a scaling parameter; the exponents n and m reflect different sensitivity on ΔK for ductile and K_{max} for quasi-brittle materials. This relationship provides the basis for the life-time prediction using the fracture mechanics approach in terms of the applied stress σ, initial a_0 and final a_c crack sizes, geometry, and properties of the material, e.g., the yield strength, σ_y, and fracture toughness, K_{1c}.
Material length scales are introduced into theoretical models of fracture [7] conventionally in two approaches: (i) as the physical length related to the microstructure of the materials (grain sizes, inclusions) and (ii) as the so-called Process Zone (PZ) length, where the physical length scale arises from scaling properties of failure. Commonly-used length scale L is given by:

$$L = \frac{1}{\pi}\left(\frac{K_c}{\sigma_u}\right)^2 \tag{2}$$

Here K_c is the fracture toughness of the material, and σ_u is its tensile strength. In fatigue problems the similar kinetic equation is used, using material constants with the relevant cyclic parameters: the crack propagation threshold ΔK_{th} and fatigue limit ΔK_c are used instead K_c and σ_u. The constant L is used in conjunction with stress-based or stress-intensity methods [2]. In these methods failure occurs when crack reaches the crack propagation threshold ΔK_{th} and the critical stress-intensity ΔK_c for crack length close to L. The physical background for the introduction of two thresholds in the term of stress intensity factor is the existence of the intermediate self-similar solution (after Irwin) for the stress field at the crack tip in elastic material, ΔK_{th} and ΔK_c. However, both limit values are the consequence of two different mechanisms in the process zone at crack tip subordinating the crack advance according to "ductile" and "quasi-brittle" scenarios. The "ductile" scenario corresponds to the Paris law of crack advance with corresponding (close to the four after Paris) power exponent. The "quasi-brittle" scenario with higher power exponent is characteristic for the final stage of fatigue crack advance or "initial material brittleness", for instance, for ceramics. There is the link between ΔK_{th} and ΔK_c thresholds, the value of the power exponent and mechanisms subordinating the staging of fatigue crack advance. The power exponents are related to the "master" mechanisms providing the free energy release at the process zone. It is in "ductile scenario" the numerous Persistent Slip Bands (PSB), when PSB correlated behavior is associated with ΔK_{th} and the four power Paris law. The following transformation of PSB into the microcrack ensembles, damage localization areas and their correlated behavior provides the ΔK_c threshold scenario of fatigue crack advance with higher power exponents. The correlated behavior of PSB and damage localization (with markings of striations) areas provides the self-similarity of crack advance in terms of ΔK_{th} and ΔK_c with characteristic power exponents. Important signs of self-similarity is the existence of self-similar solutions (mentioned in the paper) as collective PSB and damage localization modes.
Energy based length is derived using an energy balance similar to that of the Griffith theory assuming a finite amount of crack extension

$$\int_0^{2L} K^2 da = K_c^2 \cdot 2L \tag{3}$$

This theoretical conception of the FFM as the basis of the Theory of Critical Distances (TCD) is discussed in [1]. A finite amount of crack extension in FFM was introduced as conceptual theoretical basis that assumes that crack advance occurs in a discontinuous or branching dynamics with the size determined by the microstructure and deformation behavior of the material [2]. For metal fatigue L corresponds to the length of the Process Zone and is related to a microstructural parameter (the grain size) and damage localization. For quasi-brittle materials, composites L is approaching to the size of the damage localization zone [4,6,7]. In FFM the TCD conception was introduced to understand relationship of fracture in the links

with cohesive zone theory and non-locality effects to introduce two new material parameters: the distance L and $\sigma_0 >> \sigma_u$ as a characteristic strength for the materials. These parameters were used in present paper to characterize the material's brittleness, susceptibility to size effects with aim to provide a bridge between continuum-mechanics, stress-based and stress-intensity approaches and micromechanical models for different classes of materials.

INCOMPLETE SELF-SIMILARITY AND FATIGUE-CRACK GROWTH

The conception of self-similarity is developed to compare the original results concerning the role of the collective modes of defects in the power laws of fatigue crack kinetics using the assumption of the incomplete self-similarity. Interpretation of the incomplete self-similarity is based on the definition of structural scales following from the self-similar solutions for defect evolution equation and estimated under analyzing scaling invariants of fracture surface at the Process Zone.

The presentation of the crack advance in the form similar to the Paris power law reflects the links of intrinsic mechanism of crack advance and defects induced structural mechanisms of the Process Zone formation. The coherent behavior of defects in the Process Zone provides the staging of damage-failure transition and can be considered as scaling mechanism related to the incomplete similarity [8, 9]. The methodology of the incomplete self-similarity was applied to the analysis of the Paris law to describe the fatigue-crack growth as the power law:

$$\frac{da}{dN} = C\left(\Delta K\right)^m \tag{4}$$

where $\Delta K = K_{max} - K_{min}$ (K_{max} and K_{min} are, respectively, the maximum and minimum stress intensities in the fatigue cycle), and C and m are experimentally determined scaling-law constants [10]. The incomplete self-similarities assume the existence of "materials constants" related to characteristic length caused by the subordination of observable variables (da/dN and ΔK in the case of fatigue) to intrinsic structural mechanism of nonlinear damage kinetics in the Process Zone. These mechanisms are accumulated in the power exponent. Macroscopically most meaningful intrinsic variable is the length L associated with characteristic scale of the Process Zone area. The value of the power exponent m reflects the intermediate self-similar nature of damage localization providing fatigue-crack advance. The similarity parameter was introduced in [10] as:

$$Z = \frac{\sigma_y \sqrt{L}}{K_{Ic}} \tag{5}$$

Incomplete similarity (similarity of the second kind [9]) corresponds to the range $\frac{\Delta K}{K_{IC}} \ll 1$ that allows the presentation of the Paris law in the form

$$\frac{da}{dN} = C\left(\Delta K\right)^m, \quad C = \frac{\Phi_1(Z)}{\sigma_y^2 K_{Ic}^{\alpha}}, \quad m = \alpha(Z) \tag{6}$$

where α is a function of Z. Important result is that both C and m constants in the Paris law is a function of the material properties and intrinsic length L. This presentation of fatigue crack kinetics allows the explanation of experimentally measured range of the Paris law exponents that is typically between 2 and 4 for ductile materials, and approaching to 10 and more in brittle materials (intermetallics and ceramics) [10]. The fundamentally important problem is the explanation of physical mechanisms responsible for the power universality of crack advance and the nature of intrinsic length L, providing the intermediate asymptotic kinetics of the crack advance.

Physical explanation of the increase of the Paris exponent m with intrinsic length can be proposed using the similarity parameter Z. The local plasticity length ahead of the crack tip, i.e., the plastic-zone size, r_y correlates with intrinsic scales $L \sim K_{Ic}^2 / \sigma_y^2$ [5] and as the consequence, $Z \sim L / r_y$. The value of $Z \sim L / r_y$ corresponds generally to the ratio $L / r_y > 1$, illustrating the difference between the plastic-zone size r_y and the Process Zone L, containing mutual fatigue striation transforming into the Critical Distance with following crack advance. It means that Z is consistent with extensive crack-tip

plasticity which promotes crack advance via ductile striation formation and secondary (daughter) crack origin at the crack tip.

DUALITY OF SINGULARITIES IN CRACK NUCLEATION AND PROPAGATION

The explanation of the self-similarity and corresponding internal scales is based on the specific nonlinearity (metastability) of free energy of solid with defects (and corresponding free energy release). The duality of singularities of crack nucleation and propagation follows from the existence of two self-similar intermediate singular solutions: the Irwin solution for the stress field at crack tip (regular attractor) and strange attractor with dynamics determined by the set of blow-up damage localization modes (the daughter crack sizes). The duality of singularities related to internal scales was supported experimentally analyzing high speed framing of the intermittent (branching) crack dynamics and in situ stress dynamics in the preloaded PMMA plate [3, 6]. The definition of the internal scale L and the subject of damage-failure transition in fatigue can be studied starting from the classical Griffith results. According to the Griffith's theory [11] the crack resistance was introduced analyzing the sum of the energy U of elastic materials due to the energy release and the energy of the development of the new surface at the crack tip (Fig.1, curve 1)

$$U = -\frac{\sigma^2}{2E}\left(\frac{\pi a^2}{4}\right) + 2\gamma a \tag{7}$$

where γ is the surface energy; σ is the applied stress; a is the crack length; E is the elastic modulus. The Griffith conception was developed by Irwin [12]) as the force version of the crack stability based on the intermediate self-similar singular solution for the stress field at the crack tip area

$$\sigma_{ik} \approx K_I r^{-1/2} f_{ij}(\theta), \; K_I = \sigma\sqrt{\pi a} \tag{8}$$

where K_I is the stress intensity factor, r, θ are the coordinates of point, $f_{ij}(\theta)$ is the θ dependence in the first term of asymptotical solution.

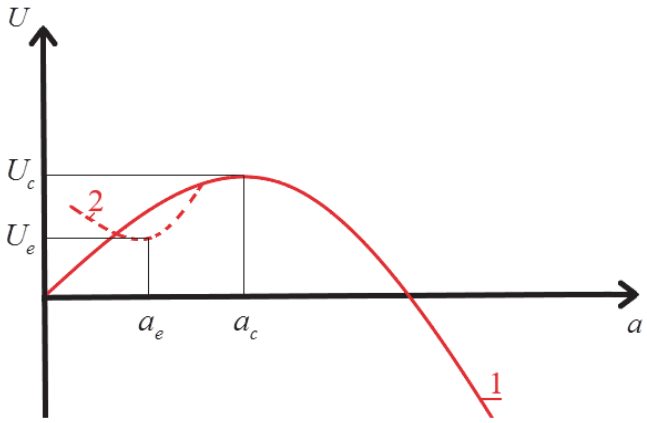

Figure 1: The Griffith (1) and Fraenkel (2) energy form of elastic solid with a crack.

Fraenkel [13] attracted the attention concerning the physical contradiction of the Griffith's (the global energy instability and singularity of stress field at the crack tip) and proposed the physically realistic form of the energy U with the local minimum $U_e(a_e)$ (Fig. 1, curve 2). The energy barrier $\Delta U = U_c - U_e$ determines the work of the stress field at the crack tip under transition from the metastable to the unstable state of crack. This energy can be estimated as $\Delta U \sim \sigma_0 L^3$ and determines the finite amplitude energy initiating critical damage over the length L. It was shown in [2, 8], that the metastable energy form, assumed by Fraenkel, has the relationship to the collective behavior of the defect ensemble in the Process Zone localized on characteristic length L providing daughter crack initiation and main crack advance. Incomplete self-similarity signs in fatigue crack advance are related to the intermediate scaling laws of damage localization kinetics [14] and can be established by statistical theory describing the damage kinetics as collective behavior of defects ensemble. The statistical theory of

mesoscopic defects (microcracks, microshears) was developed and specific type of critical phenomena in solid with defects, the structural-scaling transitions, was established [2,8]. The statistical approach and statistically based phenomenology established two "order parameters", the defect density tensor p_{ik} (defect induced strain) and the structural scaling parameter $\delta = \left\langle \left(R / d \right)^3 \right\rangle$ This parameter is responsible for the current susceptibility of solid for the defect growth and represents the mean ratio of the spacing between defects R and size of defects d. Statistically predicted non-equilibrium free energy for uniaxial case $F(p,\sigma)$ allowed the generalization of the Ginzburg-Landau phenomenology in terms of mentioned order parameters

$$F = \tfrac{1}{2} A(1 - \delta/\delta_*) p^2 - \tfrac{1}{4} B p^4 + \tfrac{1}{6} C(1 - \delta/\delta_c) p^6 - D\sigma\ p\ + \chi \left(\nabla_l p \right)^2 \tag{9}$$

where $p=p_{yy}$, $\sigma = \sigma_{yy}$ is the stress, The bifurcation points δ_*, δ_c play the role that is similar to characteristic temperatures in the Ginzburg-Landau phase transition theory. The gradient term in Eqn. (9) describes the non-local interaction in the defect ensemble; A, B, C, D are positive material parameters and χ is the nonlocality coefficient. Solution of $\partial F / \partial p = 0$ gives the "equilibrium" dependencies $p=p(\sigma,\delta)$ in different ranges of δ. These dependencies and corresponding free energy form are presented in Fig.2

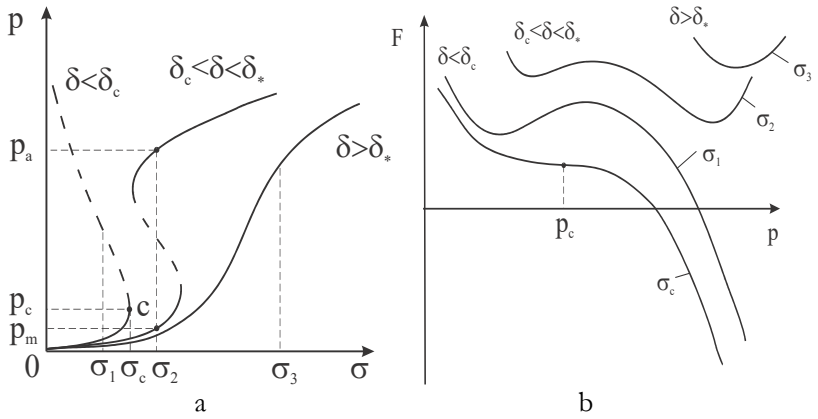

Figure 2: The "equilibrium" dependencies $p=p(\sigma,\delta)$ (a) and corresponding free energy forms (b) in different ranges of δ

Two-walls potential reflects qualitative different scenarios of defects kinetics, that follows to the evolution inequality [4]:

$$\frac{dF}{dt} = \frac{\partial F}{\partial p}\frac{dp}{dt} + \frac{\partial F}{\partial \delta}\frac{d\delta}{dt} \le 0 \tag{10}$$

and the kinetic equations for the defect density p and structural-scaling parameter δ

$$\frac{dp}{dt} = -\Gamma_p \left(A(1 - \frac{\delta}{\delta_*}) p\ - Bp^3 + C(1 - \frac{\delta}{\delta_c}) p^5 - D\sigma\ - \frac{\partial}{\partial x_l}(\chi \frac{\partial p}{\partial x_l}) \right) \tag{11}$$

$$\frac{d\delta}{dt} = -\Gamma_\delta \frac{\partial F}{\partial \delta} \tag{12}$$

where $\Gamma_p > 0$ and $\Gamma_\delta > 0$ are the kinetic coefficients.

INTERMEDIATE SELF-SIMILAR COLLECTIVE MODES OF DEFECTS

The scaling laws follow to the nonlinear dynamics of defect density tensor in the process zone and both scaling-law constants (C and m) describe the universality of critical system dynamics in term of observable variables (K_I in our case). This situation is analogous to the classical scaling laws in the phase transition theory near the critical points. It can be shown that the incomplete self-similarity in the Paris power law is the consequence of the existence of the intermediate self-similar solutions of Eqn. (11) subordinating characteristic stages of defects kinetics both ductile and quasi-brittle materials in the Process Zone. As it follows from the solution of Eqns. (11), (12) the transitions through the bifurcation points δ_c and δ_* lead to a drastic change of defects kinetics. In the range $\delta_c < \delta < \delta_*$ macroscopic modes of the defect density p_{ik} with pronounced orientation appear due to the nature of free energy metastability. Orientation transition in defect ensemble and following plastic strain localization in the form of numerous Slip Bands reveals the dynamics of solitary waves [2] $p(\zeta) = p(x-Vt)$

$$p = \frac{1}{2} p_a \left[1 - tahn(\zeta L_S^{-1})\right], \qquad L_S = \frac{4}{p_a}\left(2\frac{\chi}{A}\right)^{1/2} \tag{13}$$

where L_S is the front length of solitary waves of strain localization. The velocity of solitary wave front is expressed as $V = \chi A\left(p_a - p_m\right)/2\zeta^2$, where $(p_a\text{-}p_m)$ is a jump in the metastability area that is governed by the kinetics of structural-scaling parameter Eqn. (12). These numerous Slip Bands-SB can be considered as mesoscopic precursor of Striations, in the Plastic-Zone area with the size r_y (S_1, Fig.3).

The kinetics of the structural-scaling parameter plays the crucial role in the formation of the defect-ordered phase providing the effective mechanism of strain localization. It was shown in [15] that self-similar defects orientation kinetics according to the solution (13) subordinates the plastic zone formation on the length r_y due to the interaction of several SB areas providing the scaling with the power exponent $m\sim4$. Similar scenario is observed as the 4th power universality of plastic wave fronts in shocked materials [16]. Important feature of the power law universality is the critical behavior in defect ensemble and as the consequence the anomaly of the energy absorption in the presence of the stress singularity [17]. Dramatic changes occur in material responses due to the path of the critical point δ_c (entering into the area $\delta < \delta_c \approx 1$]. Eqn. (11) can be re-written in the vicinity of critical point p_c for the free energy release term as the power form for $p > p_c$ [2,3]

$$\frac{dp}{dt} \approx G(p_c)\, p^m + \frac{\partial}{\partial x}\left(\chi(p_c)\frac{\partial p}{\partial x}\right) \tag{14}$$

and a new type of the defect collective modes appears as the blow-up self-similar solution of Eqn. (14)

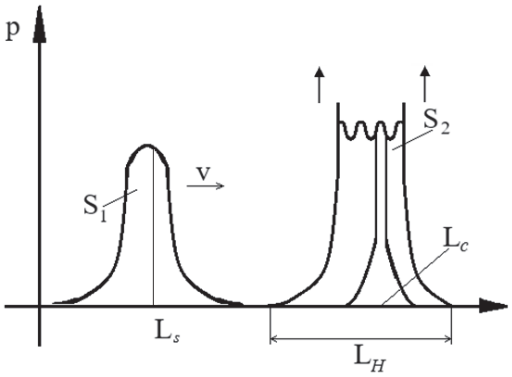

Figure 3: Self-similar solutions corresponding to solitary wave (S_1) and blow-up (S_2) collective modes of defects.

$$p = g(t)\, f(\xi),\ \xi = x/L_H,\ g(t) = G\left(1 - t/\tau_c\right)^{-m} \tag{15}$$

where τ_c is the so-called "peak time" ($p \to \infty$ at $t \to \tau_c$ for the self-similar profile $f(\xi)$ of defects localized on the scale L_H), $G > 0$, $m > 0$ are the parameters of non-linearity characterizing the free energy release for $\delta < \delta_c$. The blow-up self-similar solution Eqn. (15) describes the damage kinetics for $t \to \tau_c$, $p \to p_c$ on the set of spatial scales $L_H = kL_c$, $k=1,2\ldots K$, where L_c and L_H stand for the "simple" and "complex" blow-up dissipative structures [2]. The scale L_c represents the "quantization length" of damage localization in the process zone providing the variety of the crack paths in the presence of two singularities: intermediate asymptotic solution for stress distribution at the crack tip area and the blow-up damage localization kinetics in the process zone [6].

The free energy metastability of solid with defects in the range $\delta < \delta_c \approx 1$ (Fig.2) allows the explanation of the Fraenkel energy form (Fig.1) and the link of damage localization kinetics on the set of lengths L_H at the crack tip with transition from steady to branching crack dynamics [15].The existence of three types of self-similar solutions related to the stress intensity factor, solitary and the blow-up defects collective modes reveals the duality of the singularities providing different crack kinetics [3,15]. The interaction of the SB areas as new mesoscopic defects leads to the pass of critical point δ_c and initiation of self-similar blow-up modes on the set of lengths $L_H = kL_c$, $k=1,2\ldots K$. The blow-up modes have pronounced structural image for quasi-brittle materials as the mirror zones on the fracture surface [6].

The parameter m in Eq (15) characterizes the free energy release nonlinearity with the rate that exceeds essentially the kinetics of defects in the metastability area $\delta_c < \delta < \delta_*$ providing the set of the SB areas. It explains the high value of the power exponent in quasi-brittle material in Eqn.(1) due to the qualitative new nature of the intermediate self-similar blow-up solution for defects kinetics in comparison with self-similar solitary wave solution (13) subordinating the fatigue crack advance in ductile materials.

To follow the definitions in [18] the collective modes of defects with solitary wave and blow-up dynamics can be associated with Shear Transformation Zones (STZ) and Damage Transformation Zones (DTZ) localized on the spatial scales of corresponding self-similar solutions (13), (15).

INTERPRETATION OF THE BATHIAS-PARIS DIAGRAM

The illustration of singularities role related to the intermediate self-similar solutions (8), (13) and (15) can be given by the interpretation of the Bathias-Paris diagram of fatigue crack growth [19,20], when both, stress and stress-intensity based scenario of damage-failure transition, are presented in Fig. 4.

The diagram illustrates that short crack growth is determined by the Herzberg kinetic, which is sensitive to the structural Burgers vector parameter, and long crack advance follows to the Paris kinetic Eqn. (4). The factor x in this paper defines the transition point from short crack to long crack scenario and depends on the load ratio [20]. The transition from STZ (solitary wave) to DTZ (blow-up) kinetics is the consequence of specific nonlinearity in the presence of the metastability of free energy release and non-locality effects. This allows the explanation of transition from short crack initiation and growth to fatigue crack nucleation and propagation in terms of two limit values, ΔK_{th} and ΔK_c. Both limit values are the consequence of two different mechanisms in the process zone at the crack tip subordinating the crack advance according to "ductile" and "quasi-brittle" scenarios. The "ductile" scenario corresponds to the Paris law of crack advance with corresponding (close to the four after Paris) power exponent. The "quasi-brittle" scenario with higher power exponent is characteristic for the final stage of fatigue crack advance or "material brittleness. There is the link between ΔK_{th} and ΔK_c. thresholds, the value of the power exponents and mechanisms subordinating the staging of fatigue crack advance. The power exponents are related to the "master" mechanisms providing the free energy release at the process zone. It is in "ductile scenario" the numerous Persistent Slip Bands (PSB), when PSB correlated behavior is associated with ΔK_{th} and the four power Paris law. The following transformation of PSB into the microcrack ensembles, damage localization areas and their correlated behavior provides the ΔK_c. threshold scenario of fatigue crack advance with higher power exponents. The correlated behavior of PSB and damage localization (with markings of striations) areas provides the self-similarity of crack advance in terms of ΔK_{th} and ΔK_c with characteristic power exponents.

The ΔK- independent area of fatigue crack initiation corresponds to the DTZ kinetics with explosive jump from structure dependent scales of defects a_{int} to macroscopically recognized small cracks a_0. The power law $da/dn = b(a/a_0)^{n/2}$ reflects the self-similar (blow-up) stage of damage kinetics over the scale L_c that allows the estimation of $a_0 \sim L_c$. Starting from the scales a_0 the singularity related to the stress intensity factor ΔK is combined with STZ spatial-temporal dynamics (13), that provides numerous STZ initiation and material refining up to the scale a_1. The drop of the crack velocity is the consequence of subjection of crack kinetics to the stress intensity factor ΔK according to the Paris law. The process zone scale in this case is associated with the length $L \sim L_H$.

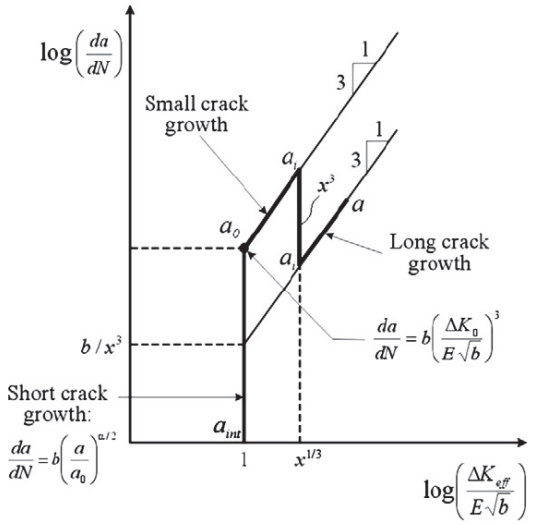

Figure 4: Crack advance diagram in HCF [19,20]: b is the Burgers vector, ΔK_0 and ΔK_{eff} are stress intensity factors corresponding to the crack lengths a_0 and a_1.

Self-similarity of fatigue damage-failure transition corresponds to self-similar pattern of fracture surface that was studied in [21] calculating spatial (scaling) invariant (the Hurst exponent) of the fracture surface roughness for the identification of characteristic lengths, associated with defects spacing l_{sc} (close to the Burgers vector b in the Bathias-Paris's diagram) and the process zone L_{PZ} related to mentioned scales r_y and L. These lengths correspond to the range of scales $[l_{sc}, L_{PZ}]$ characterizing correlated behavior of defects in the process zone L_{PZ}. Mentioned scenario can be illustrated by the morphological images of crack nucleation and propagation in the conditions of VHCF, Fig.4. Taking into account the ratio $\frac{l_{SC}}{L_{PZ}} << 1$ that is characteristic for the incomplete self-similarity the intermediate asymptotic equation for the crack velocity da/dN can be written as [17]:

$$\frac{da}{dN} = l_{sc}\left(\frac{\Delta K_{eff}}{E\sqrt{l_{sc}}}\right)^{\alpha},\ \Delta K_{eff} = \Delta K\left(\frac{L_{pz}}{l_{sc}}\right), \tag{16}$$

where α is the power exponent for the area 2 (Fig. 4) in the range of scales $[l_{sc}, L_{PZ}]$ corresponding to multiscale correlation of defect induced roughness, $K_{th} \sim E\sqrt{l_{sc}}$. The Paris law corresponds to the area 3. As it follows from (16) the constant C reads:

$$C = l_{sc}\left(\frac{L_{pz}}{l_{sc}}\right)^{\alpha} \tag{17}$$

Two scales l_{sc} and L_{PZ} were estimated analyzing the roughness of fracture surface of aluminum alloy in VHCF regime by interferometer-profiler New View 5010 to establish quantitative invariant characteristics of the fracture surface in terms of the scaling Hurst exponent [22].

SCALING INVARIANCE OF FATIGUE CRACK GROWTH IN VHCF REGIME

Fatigue crack growth tests were carried out under fully reversed tension (R = −1) in mode I, following a methodology that was similar to that prescribed in the ASTM E647 standard. The material is a non-standard hot rolled low alloy steel grade (named R5 according to the International Classification Societies of Offshore Systems) with a typical fine grain microstructure, composed of tempered martensite and bainite. This steel is used after a double quenching in water, a first period at 920 °C and a second period at 880 °C, and then tempering at 650 °C with water cooling. Following this heat

treatment, the material exhibits the following mechanical properties: hardness 317 HB, yield strength 970 MPa, ultimate tensile strength UTS = 1018 MPa, Young's modulus E = 211 GPa under monotonic quasi-static tension. The R5 high-strength steel reveals at the room-temperature the fatigue limit of 600 MPa for 10^6 cycles at 10 Hz.

Fatigue symmetric tension–compression test at 20 kHz was conducted on an ultrasonic fatigue testing machine for the R5 high-strength steel specimens (Fig. 6) with the purpose to establish damage induced scaling properties in the process zone. The testing apparatus comprised the following principal components: a generator, which transformed 50 Hz fluctuations into an ultrasonic electric sinusoidal signal with a frequency of 20 kHz; a piezoelectric transducer, which generated longitudinal ultrasonic waves and produced mechanical action at a frequency of 20 kHz; and an ultrasonic waveguide, which augmented the amplitude of mechanical stresses in the (operating) central region of the specimen. An air-cooling system is employed to prevent the sample from overheating. The stress in the center of the specimen is set by a software-controlled displacement of the free end of the specimen. The crack length is measured with an optical digital camera.

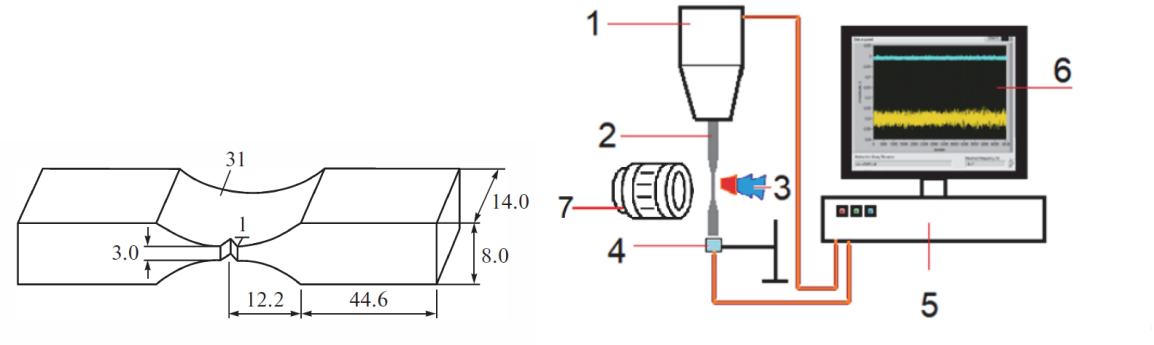

a) b)

Figure 5: Schematic picture of the specimen with lengths in mm a) and experimental setup b) 1 - horn, 2 - specimen, 3 - cooling system 4 - displacement sensor; 5 controlling and analog-digital converter system, 6 – analyzing software, 7 - camera lens for measuring crack length.

Initially the fatigue crack with a length of ~1.5 mm was initiated, and the following growth was controlled by varying the load amplitude stress intensity increment ΔK calculated by formula:

$$\Delta K = \frac{E}{(1-\nu^2)}\sqrt{\frac{\pi}{a}}A_0 Y(a/w) \tag{18}$$

where E is the Young's modulus, ν is the Poisson ratio, A_0 is the amplitude of oscillations, Y is the polynomial factor, and w is the specimen width. The polynomial factor for a given sample geometry (Fig. 5) was as follows:

$$Y(a/w) = 0.635(a/w) + 1.731(a/w)^2 - 3.979(a/w)^3 + 1.963(a/w)^4 \tag{19}$$

Following the completion of the experimental procedure, the samples were subjected to cooling in liquid nitrogen with aim to open fracture surface. Its pattern is presented in Fig. 6, which also includes images of the crack advance areas resulting from the modulation of the stress intensity factor. The change in the stress intensity factor led to the appearance of a thin trace on the fracture surface, which allowed it to be divided into three areas: 1 - small crack propagation area, 2-long crack propagation area, 3-initial crack area.

The fracture surface pattern was studied using the high-resolution profilometer (New View 5010) with a vertical resolution of 0.1 nm and a lateral resolution of 0.5 μm for determining the scaling invariants of defects induced roughness in the Process Zone (Fig.7). Two characteristic scales are assumed on the fracture surface. The first, l_{si}, is related to the length at which the defects interact to form the relief of the fatigue crack, and the second, L_{pz}, is the size of the zone in which this interaction occurs.

At each stage of the crack propagation path, three-dimensional images of a 105x1040 mm surface were taken and 13 one-dimensional profiles were analyzed.

The scaling invariant in term of the Hurst exponent H was estimated by the averaging of difference in roughness heights $z(x)$ on the Process Zone surface according to the formula [21]:

$$C(r)=\left\langle (z(x+r)-z(x))^2 \right\rangle_x^{(1/2)} \propto r^H \tag{20}$$

The log-log plot $log_2C(r) \sim log_2(r)$ allowed the estimation of the roughness exponent as a spatial invariant corresponding to a constant slope in corresponding range of scales $[l_{sc}, L_{pz}]$, (Fig.8).

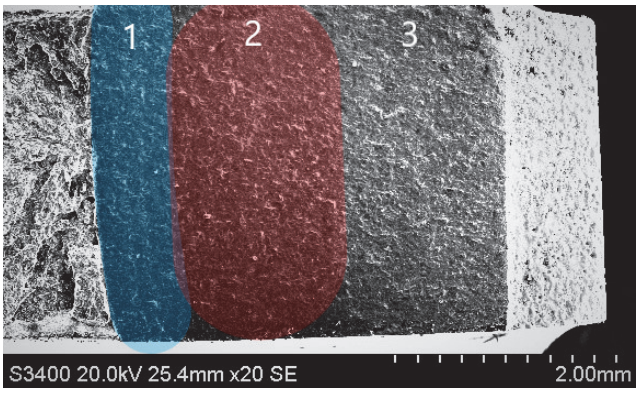

Figure 6: Fracture surface image (electronic microscopy) of the R5 steel reflecting the crack advance staging: 1 - area of small crack growth, 2 – area of long crack growth, 3 – area of initial crack.

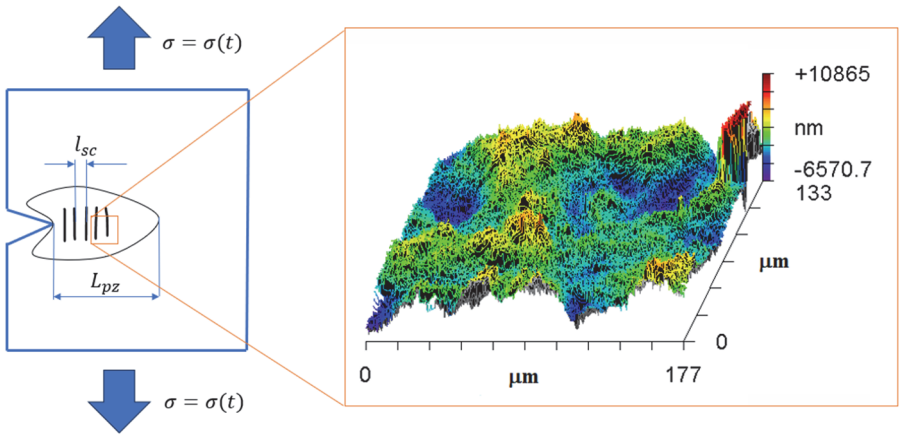

Figure 7: Schematic image of the process zone at the crack tip and typical image of the surface roughness.

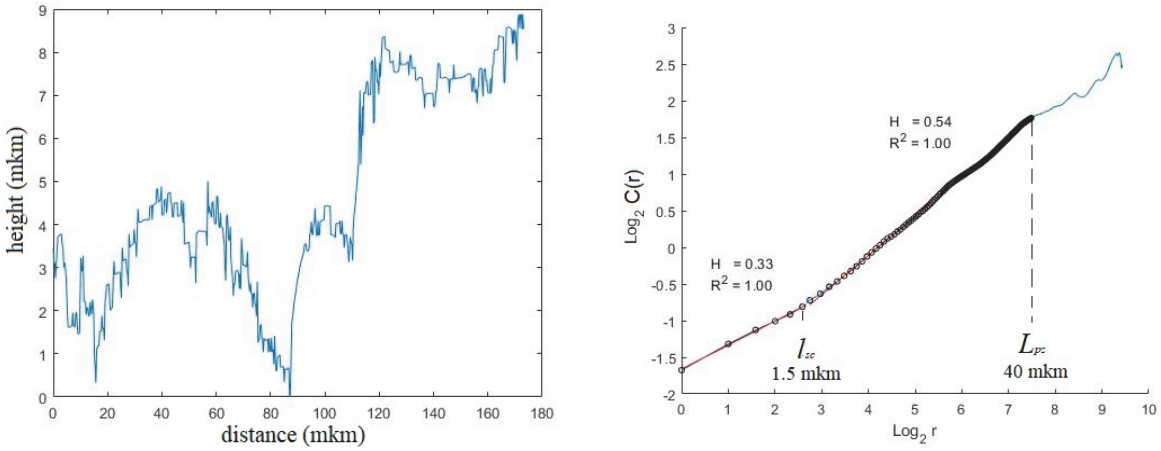

(a) (b)

Figure 8: a) The surface roughness profile, b) the $log_2C(r)$ vs $log_2(r)$ plot.

Resolution of the New View profilometer ensures the determination of upper and lower boundaries providing the power law of the roughness correlation. The value of the lower boundary of the linear section of the function C(r) was taken as the value of the critical scale l_{sc}, that is the minimum spatial scale in the Process Zone, at which scale-invariant relief patterns manifests as defect induced structural scale, the value of the upper boundary L_{pz} was taken as the length associated with the maximum area of correlated roughness behavior. The length lsc determines the so-called cross-over point separating the long-range correlation corresponding to the Paris crack advance and the Critical Distance formation with the length L_{pz} (Fig. 8b). The average values of the characteristic l_{sc} and L_{pz} values obtained from measurements on 13 cross-section profiles for various crack propagation states are presented in the Tab. 1.

ΔK, MPa$\sqrt{m}$	Δa,m	ΔN, cycles	lsc, μm	Lpz , μm	H
6.200	$6.80\cdot10^{-4}$	$2.05\cdot10^{6}$	1.7±0.8	28.2±7.5	0.41±0.04
5.890	$2.00\cdot10^{-4}$	$2.82\cdot10^{6}$	0.9±0.3	38.1±7.1	0.49±0.03
5.596	$3.20\cdot10^{-4}$	$4.74\cdot10^{5}$	1.7±0.7	34.1±8.6	0.41±0.04
5.316	$2.20\cdot10^{-4}$	$4.22\cdot10^{5}$	0.9±0.3	38.2±11.9	0.43±0.03
5.050	$2.60\cdot10^{-4}$	$7.37\cdot10^{5}$	1.3±0.5	34.1±7.3	0.44±0.03
4.797	$1.60\cdot10^{-4}$	$2.75\cdot10^{5}$	1.3±0.5	42.2±10.9	0.50±0.02
4.558	$3.20\cdot10^{-4}$	$7.13\cdot10^{5}$	1.4±0.5	31.1±4.7	0.52±0.02
4.330	$4.93\cdot10^{-4}$	$4.33\cdot10^{7}$	1.3±0.5	39.5±6.8	0.47±0.03

Table 1: Test conditions, characteristic scales l_{sc}, L_{pz} and the Hurst exponent H for different stages of crack advance.

3D New View roughness data (Fig.8) revealed the existence of two characteristic scales: the scale of process zone L_{pz} and correlation length l_{sc}, that is the scale, when correlated behavior of defect induced roughness has started. The measured l_{sc} and L_{pz} scales from Tab. 1, substituting them into Eqn.(16), allow the estimation of the power-law exponent for various stages of crack advance. The exponent α ~2.51 corresponds to the linear slop for the small crack advance defined essentially by the surrounded damage area (Fig. 9). The exponent α ~3.88 is characteristic for the Paris crack advance determined mainly by the stress intensity asymptote.

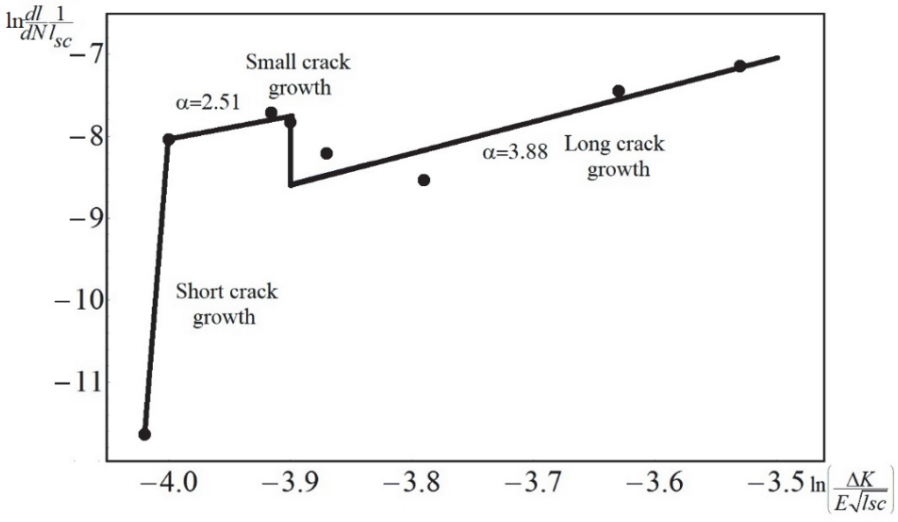

Figure 9: Characteristic plots $ln\left(\frac{dl}{dN}\frac{1}{l_{sc}}\right)$ vs $ln\left(\frac{\Delta K}{E\sqrt{l_{sc}}}\right)$ for different staging of crack advance.

Critical distance under fatigue loading of the R5 steel corresponds to the value $L_{eff} \sim L_{pz} \approx 38\ \mu m$ for the Paris crack and threshold stress intensity factor $\Delta K_{th} \approx 4.33$ MPa$\sqrt{m}$. Substituting the experimental data for L_{pz} and ΔK_{th} into Eqn. (2), the value of the fatigue limit for steel R5 can be determined. The fatigue limit obtained by this formula for steel R5 is equal to $\sigma_0 \approx 396$ MPa which is 4% more than the experimentally found fatigue limit in VHCF tests was reported in [24] ($\sigma_0 \approx$ 381 MPa, $R = -1$, in air and room temperature, $N_c \sim 10^9$ cycles). High frequency conditions of VHCF loading provides the unique opportunity to study the role of different factors and mechanisms of damage localization and crack advance. Qualitative difference of small crack and the Paris crack advance is reflected in the values of power exponents and corresponding leading mechanisms responsible for damage localization at the process zone area. Power exponent $\alpha \sim 2.51$ characterizes the leading role of the blow-up self-similar solution (5) for small crack kinetics and the dramatic changes of leading mechanisms and the power exponent $\alpha \sim 3.88$ for the Paris crack, when the damage localization in the process zone follows to the stress intensity factor at the crack tip area.

Conclusion

Thermodynamic basis of FFM was formulated as the metastability of the free energy release in solids with defects in the presence of macroscopic cracks. Statistical thermodynamics and kinetics of damage-failure transition represent generalized Ginzburg-Landau approach, that link the crack advance with generation of collective modes of defects having the nature of the intermediate asymptotic solution of the defect evolution equation. These modes have self-similar singular spatial-temporal dynamics (solitary waves as STZ and blow-up modes as DTZ) subordinating the staging of plastic strain localization and damage localization in the Process Zone area at the crack tip in the condition of specific type of critical phenomenon in solids with defects, the structural scaling transition. Two ranges of structural scaling parameter that are responsible for the current material susceptibility to defects growth correspond to qualitative different forms of free energy metastability and free energy release dynamics. The set of the STZ provides "two walls" metastability decomposition and the anomaly of the energy absorption in the Process Zone subordinating the crack advance in ductile materials with the power exponent for stress intensity factor close to 4. Drastic change of the free energy metastability (with infinite depth of the second minima predicted by Fraenkel) leads to the generation of the set of DTZ with blow-up dynamics of damage localization and the energy absorption kinetics at the Process Zone with high power exponent for stress intensity factor. Characteristic length L of the Process Zone depends on the interaction of STZ for ductile materials and DTZ for quasi-brittle materials that determines the length associated with the Critical Distances.

The interaction between STZ and DTZ was studied analyzing the correlation properties of fracture surface roughness calculating the Hurst scale invariant for ductile material. Two structural lengths were identified characterizing the range of correlated behavior of defects [l_{sc}, L_{pz}]. These structural lengths were used to determine the scaling parameter of the incomplete self-similarity, characteristic stress intensity factors $K_{th} \sim E\sqrt{l_{sc}}$, $\Delta K_{eff} = \Delta K(L_{pz}/l_{sc})$ to derive the kinetic equation for fatigue crack advance. The interpretation of the Bathias-Paris diagram was proposed using this kinetic equation and original experimental data of staging for the damage-failure transition in the condition of VHCF. The origin of small crack a_0 was identified as the blow-up collective mode (DTZ) of damage localization over L_c fundamental length. The advance of the small crack is subordinated by $K_{th} \sim E\sqrt{l_{sc}}$ up to the Paris crack length. The Paris crack advance follows to the effective stress intensity ΔK_{eff} with the power exponent close to conventional value 4.

Author contribution

Author contributions are following. Conceptualization: O.B.N. (Oleg B. Naimark); methodology V.A.O. (Vladimir A. Oborin), M.V.B. (Mikhail V. Bannikov); writing-original draft preparation: O.B.N., V.A.O., M.V.B.

Acknowledgements

The work was carried out as part of a major scientific project funded by the Ministry of Science and Higher Education of the Russian Federation (Agreement No. 075-15-2024-535 dated 23 April 2024).

REFERENCES

[1] Taylor, D., Cornetti, P. (2005). Finite fracture mechanics and the theory of critical distances, Advances in Fracture and Damage Mechanics, IV, pp. 565-570.

[2] Naimark, O.B. (2004). Defect Induced Transitions as Mechanisms of Plasticity and Failure in Multifield Continua, Advances in Multifield Theories of Continua with Substructure, Capriz, G. and Mariano, P., eds., Boston: Birkhauser, pp. 75–114.

[3] Naimark, O. (2016). Energy release rate and criticality of multiscale defects kinetics, Int. J. Fracture, 202, pp. 271–279. DOI: 10.1007/s10704-016-0161-3.

[4] Naimark, O. (2019). Duality of singularities of multiscale damage localization and crack advance: length variety in Theory of Critical Distances, Frattura ed Integrità Strutturale, 49, pp. 272-281. DOI: 10.3221/IGF-ESIS.49.27.

[5] Ritchie, R.O., Gilbert, C.J., McNaney, J.M. (2000). Mechanics and mechanisms of fatigue damage and crack growth in advanced materials, International Journal of Solids and Structures, 37, pp. 311-329.

[6] Naimark, O.B., Uvarov, S.V. (2004). Nonlinear crack dynamics and scaling aspects of fracture (experimental and theoretical study), Int. J. Fracture, 128, pp. 285-292. DOI: 10.1023/B:FRAC.0000040992.50470.8a.

[7] Ritchie, R.O. (2005). Incomplete self-similarity and fatigue-crack growth, International Journal of Fracture, 132, pp. 197–203. DOI: 10.1007/s10704-005-2266-y.

[8] Naimark, O.B. (2003). Collective Properties of Defect Ensembles and Some Nonlinear Problems of Plasticity and Fracture, Phys. Mesomech., 6(4), pp. 39–63. DOI: 10.1134/S1029959917010076.

[9] Barenblatt, G.I. (1996). Scaling, Self-Similarity, and Intermediate Asymptotics. Cambridge University Press, Cambridge, UK.

[10] Ritchie, R.O. (1999). Mechanisms of fatigue crack propagation in ductile and brittle solids, International Journal of Fracture, 100, pp. 55–83.

[11] Griffith, A.A. (1921). The phenomena of rupture and flow in solids, Phil. Trans. Roy. Soc. London, Ser. A 221, pp. 163-198.

[12] Irwin, G.R. (1957). Analysis of stresses and strains near the end of a crack traversing a plate, Journal of Applied Mechanics, 24, pp. 361-364.

[13] Fraenkel, Ya..I. (1952). Theory of reversible and non-reversible cracks in solid, Journal of Technical Physics, 22, pp. 1857-1866.

[14] Barenblatt, G.I. and Botvina, L.R. (1981). Incomplete self-similarity of fatigue in the linear range of crack growth, Fatigue of Engineering Materials & Structures, 3, pp. 193–212.

[15] Naimark, O., Bayandin, Yu., Uvarov, S., Bannikova, I., Saveleva, N. (2021). Critical Dynamics of Damage-Failure Transition in Wide Range of Load Intensity, Acta Mechanica, 232, p.p. 1943–1959. DOI: 10.1007/s00707-020-02922-1

[16] Naimark, O.B., Bayandin, Yu.V., Zocher, M.A. (2017). Collective properties of defects, multiscale plasticity, and shock induced phenomena in solids, Physical Mesomechanics, 20, pp.10-30. DOI: 10.1134/S1029959917010027.

[17] Naimark, O. (2019). Duality of singularities of multiscale damage localization and crack advance: length variety in Theory of Critical Distances, Frattura ed Integrità Strutturale, 13 (49), pp. 272-281. DOI: 10.3221/IGF-ESIS.49.27.

[18] Langer, J. S (2004). Dynamics of shear-transformation zones in amorphous plasticity: Formulation in terms of an effective disorder temperature, Phys. Rev. E ,70, 041502.

[19] Bathias, C., Paris, P.C. (2005). Giga\cycle fatigue in mechanical practice, Marcel, Dekker Publisher Co.

[20] Marines-Garcia, I., Paris, P.C., Tada, H., Bathias, C., Lados, D. (2008). Fatigue crack growth from small to large cracks on very high cycle fatigue with fish-eye failures, Engineering Fracture Mechanics, 75(6), pp. 1657-1665. DOI: 10.1016/j.engfracmech.2007.05.015.

[21] Oborin, V.A., Bannikov, M.V., Naimark, O.B., Palin-Luc, T. (2010). Scaling invariance of fatigue crack growth in gigacycle loading regime, Technical Physics Letters, 36 (11), pp. 1061-1063. DOI: 10.1134/S106378501011026X.

[22] Froustey, C., Naimark, O., Bannikov, M., and Oborin, V. (2010). Microstructure Scaling Properties and Fatigue Resistance of Pre-strained Aluminium Alloys (Part 1: AleCu Alloy), Eur. J. Mech. A. Solid, 29, pp. 1008–1014. DOI: 10.1016/j.euromechsol.2010.07.005

[23] Naimark, O., Oborin, V., Bannikov, M., Ledon, D. (2021). Critical Dynamics of Defects and Mechanisms of Damage-Failure Transitions in Fatigue, Materials, 14(10), pp. 2554. DOI: 10.3390/ma14102554

[24] Bannikov, M.V., Naimark, O.B., Oborin, V.A. (2016). Experimental investigation of crack initiation and propagation in high- and gigacycle fatigue in titanium alloys by study of morphology of structure, Fract. Integr. Strutt., 10 (35), pp. 50-56. DOI: 10.3221/IGF-ESIS.35.06

[25] Pérez-Mora, R., Palin-Luc, T., Bathias, C., Paris, P.C. (2015). Very high cycle fatigue of a high strength steel under sea water corrosion: A strong corrosion and mechanical damage coupling, International Journal of Fatigue, 74, pp. 156-165. DOI: 10.1016/j.ijfatigue.2015.01.004

NOMENCLATURE

N : Number of cycles;
a : Crack length;
K_I : Stress intensity factor;
ΔK : Range of stress intensity factor;
K_{max} : Stress intensity value at maximum applied stress;
ΔK_{th} : Crack propagation threshold;
K_c : Fracture toughness;
C : Scaling parameter;
α, m, n : Experimentally determined constants;
σ_y : Yield strength;
K_{1c} : Fracture toughness;
σ_u : Tensile strength;
E : Young's modulus;
L : Length scale;
Z : Similarity parameter;
r_y : Plastic-zone size;
U : Energy of elastic materials;
γ : Surface energy;
σ : Applied stress;
θ : Coordinates of point;
p_{ik} : Defect density tensor;
δ : Structural scaling parameter;
$F(p,\sigma)$: Free energy for uniaxial case;
A, B, C, D : Positive material parameters;
χ : Nonlocality coefficient;
lsc : Scale related to the correlated behavior in the ensemble of defects;
L_{pz} : Scale associated with the process zone;
b : Burgers vector;
$C(r)$: Correlation function;
H : Hurst exponent;
$z(x)$: Surface relief height;
r : Size of window;
ν : Poisson's ratio;
A_0 : Amplitude of oscillations;
w : Specimen width;
Y : Polynomial factor;